

Topological self-organization of strongly interacting particles

Ioannis Klefogiannis¹ and Ilias Amanatidis²

¹*Physics Division, National Center for Theoretical Sciences, Hsinchu 30013, Taiwan*

²*Department of Physics, Ben-Gurion University of the Negev, Beer-Sheva 84105, Israel*

(Dated: September 12, 2019)

We investigate the self-organization of strongly interacting particles confined in 1D and 2D. We consider hardcore bosons in spinless Hubbard lattice models with short-range interactions. We show that many-body states with topological features emerge at different energy bands separated by large gaps. The topology manifests in the way the particles organize in real space to form states with different energy. Each of these states contains topological defects/condensations whose Euler characteristic can be used as a topological number to categorize states belonging to the same energy band. We provide analytical formulas for this topological number and the full energy spectrum of the system for both sparsely and densely filled systems. Furthermore, we analyze the connection with the Gauss-Bonnet theorem of differential geometry, by using the curvature generated in real space by the particle structures. Our result is a demonstration of how states with topological characteristics, emerge in strongly interacting many-body systems following simple underlying rules, without considering the spin, long-range microscopic interactions, or external fields.

I. INTRODUCTION

Self-organization mechanisms occurring in many-body systems, that result in novel phases of matter, are one of the most important pursuit in physics. One of the most celebrated examples is a universal mechanism of phase transitions, based on breaking of symmetries, invented by Landau¹ and expanded by others, to describe long-range ordering phenomena like, ferromagnetism and solid, liquid and vapour transitions. Moreover, this universal mechanism has been successfully applied to describe phases formed under extreme conditions like, superconductivity and superfluidity. The key ingredient in Landau's theory is local order parameters that take different values between the different phases of matter, according to the relevant symmetries present. Later, other important self-organization mechanisms related to topology were discovered, that do not require long-range ordering, breaking of symmetries or order parameters²⁻¹¹. The resulting phases have been dubbed topological orders. Apart from classical systems like superfluid films^{2-6,12,13}, topological orders can manifest also in the ground states of quantum systems with a large number of interacting particles, at low temperatures, where quantum effects play an important role⁸⁻¹¹. Celebrated examples include quantum liquids like in the fractional quantum Hall effect FQHE^{14,15} and spin liquids¹⁶⁻¹⁸. For such systems, topological order is strongly tied to quantum correlations between the different components of the system, known as entanglement¹⁹⁻²³. In order to characterize topologically ordered phases, usually, a global measure that takes into account the overall spatial properties of the system has to be used. Widely used topological measures are for example, the winding number in the classical case³, or the topological entanglement entropy²⁴ and the entanglement spectrum in the quantum case²⁵⁻²⁸. Topological order is an important paradigm, showing that self-organization mechanisms leading to states of matter, are not necessarily related to long-range ordering and break-

ing of symmetries, as described in Landau's theory.

In this paper we study how strongly interacting particles self-organize to create many-body states with topological characteristics in 1D and 2D, based on simple microscopic rules. We demonstrate this by using partially filled Hubbard models with short-range interactions. For strong interaction strength, the particles organize in different sets of microstates. We show that all microstates with the same energy can be described by a topological number, the Euler characteristic of the network/graph structures formed by the empty or occupied space in the system. We calculate geometrically this topological number along with the energy spectrum of the system, for sparsely and densely filled systems, by using the topological defects/condensations contained in the microstates. Furthermore we discuss the connection with the Gauss-Bonnet theorem of differential geometry, by using the curvature generated by these topological structures.

II. MODEL

In order to demonstrate the topological self-organization mechanism we consider spinless particles in 2D Hubbard lattices or chains with short-range interactions, described by the Hubbard-like Hamiltonian

$$\begin{aligned} H &= H_U + H_t \\ H_U &= U \sum_{x=1}^{M_x} \sum_{y=1}^{M_y} (n_{x,y} n_{x+1,y} + n_{x,y} n_{x,y+1}) \\ H_t &= t \sum_{x=1}^{M_x} \sum_{y=1}^{M_y} (c_{x+1,y}^\dagger c_{x,y} + c_{x,y+1}^\dagger c_{x,y} + h.c.) \end{aligned} \quad (1)$$

where c_{xy}^\dagger, c_{xy} are the creation and annihilation operators for spinless particles at site with coordinates x,y in the lattice, while $n_{x,y} = c_{x,y}^\dagger c_{x,y}$ is the number operator. Also $M_x(M_y)$ is the number of sites along $x(y)$ giving

the total number of sites in the system $M = M_x M_y$. Schematically, we represent occupied/unoccupied sites with filled(empty) circles. When two particles occupy adjacent sites in the lattice they interact with energy U via the term H_U in Eq. 1. This short-range interaction leads to topological structures in the particle arrangements in real space, as we shall show in the following section. The interaction strength U can be either positive or negative for repulsive or attractive interaction, respectively. All energies E in the paper are expressed in units of U . A small nearest-neighbor hopping t with $|U| \gg t$, described by H_t can be treated perturbatively. In order to avoid edge effects we close our system in both directions x and y by applying periodic boundary conditions (PBC) so that the summation indices in Eq. 1 follow $M_x + 1 = 1$ and $M_y + 1 = 1$ giving $c_{M_x+1,y} = c_{1,y}$ and $c_{x,M_y+1} = c_{x,1}$. For our study we consider hardcore bosons whose many-body wavefunctions stay symmetric under exchange of two particles, but the particles cannot occupy the same quantum state. In this case only one particle is allowed per site and n_i can be either 0 or 1. The hardcore bosons satisfy the commutation relation $[c_i, c_j^\dagger] = (1 - 2n_i)\delta_{ij}$. They^{29–32} can be realized in cold atom and helium-4 systems experimentally^{23,33,34}. In overall our system corresponds to spinless hard-core bosons with strong short-range interactions on the surface of a torus. However our results could be extended to fermions and other types of particles corresponding to different occupation numbers, as the physical mechanism that generates the topological structures in the real space of the system is independent of the type of particles.

In order to characterize the topological structures in our system, we use the Euler characteristic from graph theory and differential geometry. It is defined as

$$\chi = V - E \quad (2)$$

where V is the number of vertices and E the corresponding number of edges between these vertices in the graph.

III. EULER CHARACTERISTIC AND ENERGY SPECTRUM

At the strong interaction (Mott) limit $|U| \gg t$, the particles localize at each site of the Hubbard lattice. For $t = 0$, by keeping only the interaction term H_U in Eq. 1, the microstates of the system and their corresponding energy are determined by the way the particles organize in real space. The energy of each microstate is determined by the number of particle pairs, formed when two particles occupy adjacent sites, or alternatively by the structure formed by the unoccupied sites (holes) in the lattice. The particles form what is known as charge density wave(CDW) states. A first nearest-neighbor hopping described by H_t in Eq. 1 will cause strong mixing of the states for $t = 0$. However, other types of hoppings can preserve the states for $t = 0$. We give some examples at the end of this chapter after analyzing the $t = 0$ case.

Different particle configurations/microstates can result in the same energy for $t = 0$ or belong to the same energy band when t has a small non-zero value. In short, the interaction between the particles splits the Hilbert space of the non-interacting system ($U=0$) in sub-spaces containing different many-body orders. We have found that each of these sub-spaces can be characterized by a topological number. For dense systems, the empty space between the particles forms 2D network/graph structures, whose Euler characteristic χ can be used as a topological number to characterize the respective microstates. In the rest of the paper we refer to these structures as topological defects, which are also the driving mechanism in the Berezinskii-Kosterlitz-Thouless(BKT) transition³, the prime example of topological order in classical systems. The self-organization mechanism for $t = 0$ is valid for both classical and quantum systems. However in the quantum case the system lies in a superposition of the microstates allowed at this energy. This could be considered as a simplified version of a quantum field, i.e., a coherent superposition of states with point-particles arranged at different spatial configurations.

In the rest of the current section we analyze the 2D system which concerns the major results of our paper. In Fig. 1 we show a few examples of some microstates containing different kinds of topological defects, along with their corresponding energy and the Euler characteristic, for a square system consisting of $M = 36$ sites and $N = 30$ particles. We define $L = M - N$ as the number of unoccupied sites (holes). The simplest application of our idea is to notice that changing the position of the defects, without deforming them, does not affect the total energy of the system. A simple example of this when the defects are single holes, can be seen in Fig. 1a. Furthermore, the energy does not change, if the defects are deformed in a way that maintains the total Euler characteristic of their structure (Eq. 2). This can be seen in Fig. 1b,c for example. Also, we notice that the number of defects does not change for microstates with the same energy, unless there are loops in the defects. This already hints the topological character of the many-body orders, as the defects could be considered as holes in a 2D surface/manifold.

We can derive analytical formulas for dense systems ($L \ll N$) as follows. For a dense system, the minimum energy of the system E_{min} is achieved when all the unoccupied sites are disconnected. Since each one of these holes has four nearest neighbors, it reduces the total energy of the system by

$$E_{min}^d = 4L. \quad (3)$$

In general the energy of each microstate can be calculated by subtracting this defect energy E^d , from the energy the system would have if all its sites were occupied, that is, for a full system. This energy is $E_{full} = (M_x - 1)M_y + (M_y - 1)M_x + (M_x + M_y)$, where $M_x(M_y)$ the number of sites along $x(y)$ with $M = M_x M_y$, giving

$$E_{full} = 2M. \quad (4)$$

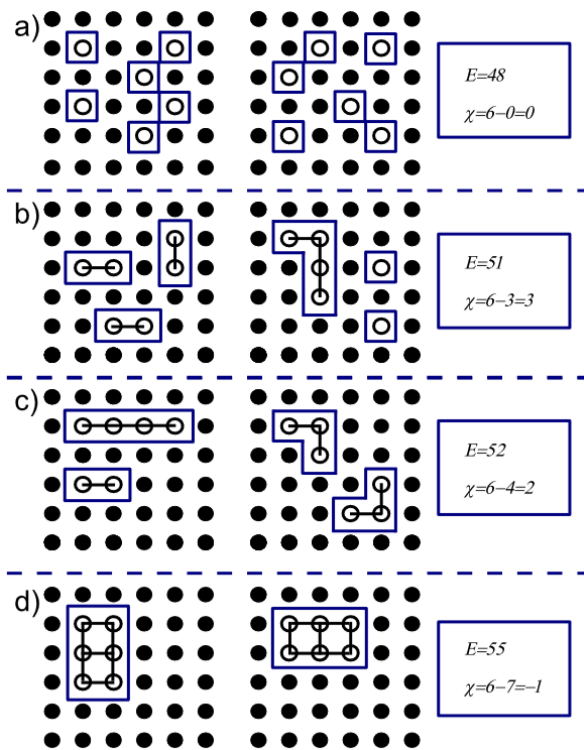


FIG. 1. Some particle configurations (microstates) for a system with $M = 36$ sites and $N = 30$ particles, at different energies. The empty space between the particles creates topological defects (blue boxes), whose Euler characteristic χ is the same for microstates with the same energy. a) All the defects consist of single unoccupied sites that are disconnected. This gives the lowest energy of the system $E_{min} = 48$, geometrically corresponding to a graph with six vertices and no edges with $\chi_{max} = 6$. b) Three topological defects can be seen which can be deformed maintaining the same energy as long as χ of their total structure is preserved. c) Same as b) but with two topological defects. d) When all the unoccupied sites are connected the maximum energy of the system is achieved $E_{max} = 55$ which corresponds geometrically to the minimum Euler $\chi_{min} = -1$ having the maximum edges between the vertices in the graph.

Then we can calculate the minimum (maximum) energy of the system from

$$E_{min(max)} = E_{full} - E_{min(max)}^d. \quad (5)$$

The corresponding microstates which are the ground states of the system, can be described by an Euler characteristic when in geometrical terms there are only L unconnected vertices and no edges. This is the maximum value of the Euler characteristic

$$\chi_{max} = L. \quad (6)$$

Also we observe that $E_{min}^d = 4\chi_{max}$.

As the individual defects/vertices become connected, the energy of the system will be increased by a single

step of U for every successive set of microstates corresponding to the excited states. On the other hand the corresponding Euler characteristic will be decreased by one, as edges between the vertices are added until the minimum Euler χ_{min} is reached corresponding to the maximum energy E_{max} of the system. This is achieved when all the holes become connected by arranging in a lattice of parallelogram shape as in Fig. 1d, for example. Any additional holes that do not fit in this parallelogram, will be arranged in a way that maximizes the connections in the overall shape of the defect. This mechanism will result in a shape with the minimum number of holes with only one connection to the parallelogram (dangling bonds). In geometrical terms this mechanism gives the maximum number of edges between the vertices. Using this idea we can derive analytical formulas for both E_{max} and χ_{min} as follows. We define $L_x(L_y)$ as the number of vertices along $x(y)$ with $L = L_x L_y$. Then the Euler characteristic of this parallelogram lattice is $\chi = L - [(L_x - 1)L_y + (L_y - 1)L_x] = -L + (\frac{L}{L_y} + L_y)$. By minimizing this expression in respect to L_y we get

$$\chi_{min} = \text{Int}[2\sqrt{L} - L]. \quad (7)$$

Following a similar approach we can calculate the maximum energy of the system by subtracting from the total energy of the system the energy removed by the defects $2L + (\frac{L}{L_y} + L_y)$. Again by minimizing this expression in respect to H_y we get $E_{max}^d = \text{Int}[2(\sqrt{L} + L)]$ which can be expressed in terms of χ_{min} as

$$E_{max}^d = \chi_{min} + 3L. \quad (8)$$

The maximum energy of the system is $E_{max} = E_{full} - E_{max}^d$. In conclusion the system is split in different energy bands determined by

$$E = E_{min}, E_{min} + 1, \dots, E_{max} \quad (9)$$

with corresponding Euler characteristic

$$\chi = \chi_{max}, \chi_{max} - 1, \dots, \chi_{min}. \quad (10)$$

with $E_{min}, E_{max}, \chi_{min}, \chi_{max}$ given by Eq. (3-8). Alternatively we can say that the energy of the system is determined by $E = 5N - 3M + \chi$ in terms of M, N, χ .

When the system is densely filled, like the cases we considered, it is reasonable to use its empty space in order to define the Euler characteristic. However, an alternative but equivalent way to characterize the microstates would be to consider the Euler characteristic of the structure formed by the occupied sites in the Hubbard lattice. This is more useful when examining a sparsely filled system for $L \gg N$. In this case the minimum energy of the system is $E_{min} = 0$ when all the particles are far apart from each other corresponding to $\chi_{max} = N$. As the particles start occupying neighboring sites, forming topological condensations, the energy of the system will be increased by one step of U for each set of microstates with higher

energies. The full energy spectrum and the corresponding Euler numbers will be given by Eq.9 and Eq.10 with $E_{max} = \text{Int}[2(N - \sqrt{N})]$ and $\chi_{min} = \text{Int}[2\sqrt{N} - N]$.

We remark that the topological defects are equivalent to the structures formed in a Hubbard model with attractive interactions ($-U$) and L particles distributed in M sites (doing a particle-hole exchange in the original system). This is an alternative way to generate the topological structures that we have presented.

When the system is in a superposition of states belonging to same energy band, long-range spatial correlations arise. In this state, all topological defects are correlated with each other, since any deformation of their patterns should maintain the total Euler characteristic. These correlations are independent of the distance between the defects. In this sense, the topological structures in our model can be thought as patterns of quantum correlations, which resemble the entanglement patterns in topologically ordered quantum many-body systems.

We cannot smoothly deform microstates with different Euler, between each other without closing the energy gaps, that is, without turning off the interaction between the particles ($U = 0$). Therefore, each set of microstates, could be considered as a different topological state, characterized by the Euler number of the corresponding particle structures.

The analysis we presented so far is valid for vanishing hopping term between the sites of the Hubbard lattice ($t = 0$ in Eq. 1). For finite nearest-neighbor hopping a strong mixing between the states will occur leading to different superpositions of the Fock states than the ones we have analyzed. However, the microstates for $t = 0$ can be preserved by considering a hopping that respects certain permutational symmetries satisfied by these states. For example, in order to preserve the internal structure of the ground states, that contain single unconnected holes, we can consider a hopping

$$H_t = t \sum_{x=1}^{M_x} \sum_{y=1}^{M_y} (N_l c_{x+1,y}^\dagger c_{x,y} N_r + N_u c_{x,y+1}^\dagger c_{x,y} N_d + h.c.). \quad (11)$$

$N_r = n_{x+2,y} n_{x+1,y+1} n_{x+1,y-1}$, $N_l = n_{x-1,y} n_{x,y+1} n_{x,y-1}$, $N_u = n_{x,y+2} n_{x+1,y+1} n_{x-1,y+1}$, $N_d = n_{x,y-1} n_{x+1,y} n_{x-1,y}$ check for holes in the right, left, up and down direction, in respect to a hole lying at coordinates x, y in the lattice. This term prevents the clustering of the single holes in the ground state. Similar hopping terms can be considered in order to preserve the topological structures formed by the particles at higher energies. These hoppings should prevent the clustering of the corresponding defect structures formed by the connected holes.

IV. CURVATURE

The structures of the topological defects/condensations generate a curvature at each

site of the Hubbard lattice that can be used to calculate the Euler characteristic of each microstate. If we use the defects, then the curvature at each site/vertice can be defined as^{35,36}

$$K(x, y) = 1 - \langle n_{x,y} \rangle - \frac{d(x, y)}{2} \quad (12)$$

where $\langle n_{x,y} \rangle$ is the occupation probability at site with coordinates x, y in the Hubbard lattice. The number of unoccupied neighboring sites $d(x, y)$ is

$$d(x, y) = f(y_+) + f(y_-) + f(x_+) + f(x_-) \quad (13)$$

with

$$\begin{aligned} y_+ &= \langle n_{x,y} \rangle + \langle n_{x,y+1} \rangle \\ y_- &= \langle n_{x,y} \rangle + \langle n_{x,y-1} \rangle \\ x_+ &= \langle n_{x,y} \rangle + \langle n_{x+1,y} \rangle \\ x_- &= \langle n_{x,y} \rangle + \langle n_{x-1,y} \rangle \end{aligned} \quad (14)$$

and $f(v) = 1 - H(2v - 1)$ where H is the Heaviside step function which obeys, $H(v) = 0$ for $v < 0$ and $H(v) = 1$ for $v \geq 0$. Notice that $K(x, y) = 0$ for occupied sites in the lattice ($\langle n_{x,y} \rangle = 1, f(v) = d(x, y) = 0$) and that the curvature takes only five values ($K(x, y) = -1, -1/2, 0, 1/2, 1$) depending on the number of neighbors for each hole in the network. The curvature can be interpreted as a local defect energy at each site. The Euler characteristic can be calculated by summing the curvature over all sites of the Hubbard lattice

$$\chi = \sum_{x=1, y=1}^{x=M_x, y=M_y} K(x, y). \quad (15)$$

This is analogous to the integration of the curvature of a closed geometrical shape (Euclidean manifold) over its surface in the Gauss-Bonnet theorem of differential geometry. The result of this integration is always $2\pi\chi$ with $\chi = 2 - 2g$ where g is the genus counting the number of holes in the geometrical shape. Shapes with the same g are topologically equivalent. In our example, not all microstates with the same χ , belonging to the same energy band, are topologically equivalent with each other. This is due to the fact that there might exist states with closed defects, containing loops which are not topologically equivalent to open defect structures. Therefore at each energy there are subsets of microstates that follow the same topology, in the sense that the defects contained in them, can be deformed continuously between each other.

Nevertheless, still the overall structure of the system in real space has to be taken into account, in order to describe its physical properties. This is a common characteristic of many topological phases of matter.

In addition, since the system contains quantum correlations between the topological defects/condensations, an extension of our approach, could provide insights into the relation between entanglement and curvature in many-body systems.

V. 1D SYSTEM

In the following we briefly analyze the respective topological structures formed in a Hubbard chain. In this case the characterization of the many-body states is much easier to obtain since the particles form structures only in a single direction. As in the 2D case we can use the Euler characteristic to describe the structure of the topological defects formed by the unoccupied sites in the lattice. The minimum energy of the system occurs when all the unoccupied sites are disconnected. It can be calculated by subtracting the energy removed by the topological defects from the energy of the system if all its sites were occupied. This gives $E_{min} = 2N - M$ for $N > M/2$ and $E_{min} = 0$ for $N \leq M/2$. The corresponding maximum Euler of the topological defects will be simply $\chi_{max} = M - N$. On the other hand when all the unoccupied sites or the particles become connected in a line, the maximum energy $E_{max} = N - 1$ and minimum Euler $\chi_{min} = 1$ are achieved. In summary the 1D system can be described by Eq.9 and Eq.10, as for the 2D system, but with $E_{min}, E_{max}, \chi_{min}, \chi_{max}$ given above. The corresponding curvature at each site, whose integration over the whole chain will give the Euler number, can be easily obtained by Eq. (12-15) after removing the terms corresponding to the y direction (y_+, y_-), resulting only in two possible values $K=0$ or $K=1$.

VI. SUMMARY AND CONCLUSIONS

We have shown how the self-organization of strongly interacting particles in 1D and 2D, with simple underlying rules, can give rise to many-body states with topo-

logical features. The topology manifests in the structures formed by the particles in real space, at different energies. Consideration of the whole system is required to get a complete understanding of its physical properties. Each set of microstates belonging to the same energy band can be described by a topological number. For a dense system we have used the Euler characteristic of the defect structures formed by the empty space between the particles. For a sparse system the corresponding Euler of the condensations formed by the occupied space in the system can be used instead. A curvature is generated by these topological defects/condensations that can be integrated over the whole real space of the system to obtain the Euler characteristic, as in the Gauss-Bonnet theorem of differential geometry. Our results show how states with topological characteristics emerge in partially filled many-body systems with strong short-range interactions.

We hope that our findings motivate further investigation of the physical mechanisms that create states with topological features and other relevant emergent phases in many-body systems, using simple microscopic rules. Apart from their fundamental significance, such mechanisms could be realized in cold atom experiments, to design novel phases of matter with various tunable properties, which are a crucial step towards the realization of quantum information applications.

ACKNOWLEDGMENTS

We are thankful to Vladislav Popkov and Daw-Wei Wang for useful comments. We acknowledge resources and financial support provided by the National Center of Theoretical Sciences in Hsinchu of R.O.C. Taiwan and the Center for Theoretical Physics of Complex Systems in Daejeon of Korea under the project IBS-R024-D1,

-
- ¹ L. D. Landau, Zh. Eksp. Teor. Fiz. 7, pp. 19732 (1937)
² V. L. Berezinskii, Sov. Phys. JETP, 32 (3): 493?500 (1971); Sov. Phys. JETP, 34 (3): 610?616 (1972)
³ J. M. Kosterlitz, D. J. Thouless, J. Phys. C: Solid State Phys. **6**, 1181 (1973)
⁴ D. J. Bishop, J. D. Reppy, Phys. Rev. Lett. **40** 1727 (1978)
⁵ V. Ambegaokar, B. I. Halperin, D. R. Nelson, E. D. Siggia, Phys. Rev. Lett. **40**, 783 (1978)
⁶ G. Agnolet, D. F. McQueeney, J. D. Reppy, Phys. Rev. B **39**, 8934 (1989)
⁷ F. D. M. Haldane, Phys. Lett. A **93**, 464 (1983a)
⁸ X.-G. Wen, Phys. Rev. B **44**, 2664 (1991)
⁹ X. Chen, Z.-C. Gu, Xiao-Gang Wen, Phys. Rev. B **82**, 155138 (2010)
¹⁰ M. Levin, X.-G. Wen, Phys. Rev. Lett. **96**, 110405 (2006)
¹¹ X. Chen, Z.-C. Gu, X.-G. Wen, Phys. Rev. B **83**, 035107 (2011)
¹² L. Mathey, K. J. Günter, J. Dalibard, A. Polkovnikov, Phys. Rev. A **95**, 053630 (2017)
¹³ R. T. Scalettar, E. Y. Loh, J. E. Gubernatis, A. Moreo, S. R. White, D. J. Scalapino, R. L. Sugar, E. Dagotto, Phys. Rev. Lett. **62**, 1407 (1989)
¹⁴ D. C. Tsui, H. L. Stormer, A. C. Gossard, Phys. Rev. Lett. **48**, 1559 (1982)
¹⁵ R. B. Laughlin, Phys. Rev. Lett. **50**, 1395 (1983)
¹⁶ B. Yoshida, Phys. Rev. B **88**, 125122 (2013)
¹⁷ S. V. Isakov, M. B. Hastings, R. G. Melko, Nature Physics **7**, 772-775 (2011)
¹⁸ L. Savary, L. Balents, Rep. Prog. Phys. **80**, 016502 (2017)
¹⁹ L. Amico, R. Fazio, A. Osterloh, V. Vedral, Rev. Mod. Phys. **80**, 517 (2008)
²⁰ R. Horodecki, P. Horodecki, M. Horodecki, and K. Horodecki Rev. Mod. Phys. **81**, 865 (2009)
²¹ A. Hamma, R. Ionicioiu and P. Zanardi Phys. Rev. A **71**, 022315 (2005)
²² I. H. Kim Phys. Rev. Lett. **111**, 080503 (2013)
²³ R. Islam, R. Ma, P. M. Preiss, M. E. Tai, A. Lukin, M. Rispoli, and M. Greiner (2015) Nature **528**, 77
²⁴ A. Kitaev, J. Preskill, Phys. Rev. Lett. **96**, 110404 (2006)

- ²⁵ H. Li, F. D. M. Haldane, Phys. Rev. Lett. **101**, 010504 (2008)
- ²⁶ V. Alba, M. Haque, A. M. Luchli, Phys. Rev. Lett. **110**, 260403 (2013)
- ²⁷ P. Calabrese, A. Lefevre, Phys. Rev. A **78**, 032329 (2008)
- ²⁸ F. Pollmann, A. M. Turner, E. Berg, M. Oshikawa, Phys. Rev. B **81**, 064439 (2010)
- ²⁹ H. M. Guo Phys. Rev. A **86**, 055604 (2012)
- ³⁰ Y.-F. Wang, Z.-C. Gu, C.-D. Gong, D. N. Sheng, Phys. Rev. Lett. **107**, 146803 (2011)
- ³¹ N.G. Zhang, C.L. Henley, Phys. Rev. B **68**, 014506 (2003)
- ³² C. N. Varney, K. Sun, M. Rigol, V. Galitski Phys. Rev. B **82**, 115125 (2010)
- ³³ R.N. Goldman, J. C. Budich, P. Zoller, Nat. Phys. **12**, 639 (2016)
- ³⁴ I. Bloch, J. Dalibard, S. Nascimbne, Nature Phys. **8**, 267-276 (2012)
- ³⁵ B. Chen, G. Chen, Gauss-Bonnet formula, finiteness condition, and asymptotic characterization for graphs embedded in surfaces, Graphs Combin. **24**, 159–183 (2008)
- ³⁶ O. Knill, A discrete Gauss-Bonnet type theorem (2010) Elemente der Mathematik, 67,1, pp1-44, (2012), arXiv:1009.2292[math.GN]; O. Knill (2011) A graph theoretical Gauss-Bonnet-Chern theorem, arXiv:1111.5395[math.DG]